reactions

MDPI

Article

Support Effects in Hydrogenation Catalysis Using Low-Loading Pd and Rh Catalysts

Stefano Paganelli [1,2,*], Oreste Piccolo [3,†], Ludovico Scarpa [1] and Alessandro Di Michele [4]

[1] Department of Molecular Sciences and Nanosystems, Ca' Foscari University of Venice, via Torino 155, 30172 Mestre (VE), Italy
[2] Interuniversity Consortium on Chemical Reactivity and Catalysis (CIRCC), Via Celso Ulpiani 27, 70126 Bari, Italy
[3] Scientific Consultancy (SCSOP), Via Trento 35, 53100 Siena, Italy
[4] Department of Physics and Geology, University of Perugia, Via Pascoli, 06123 Perugia, Italy
* Correspondence: spag@unive.it; Tel.: +39-041-2348592
† Deceased on 24 March 2026.

Abstract

A sustainable and scalable one-pot impregnation protocol, avoiding high-temperature calcination/activation, was employed to prepare Pd/Al_2O_3 (0.24 wt%), Pd/TiO_2 (0.18 wt%), Pd/ZrO_2 (0.21 wt%), Pd/SiO_2 (0.37 wt%), Rh/Al_2O_3 (0.18 wt%), and Rh/TiO_2 (0.15 wt%). Support effects on activity, selectivity, and recyclability of these low-metal content heterogeneous catalysts were investigated, using (E)-cinnamaldehyde and levulinic acid as probe molecules. In cinnamaldehyde hydrogenation, Pd catalysts were highly effective for chemoselective C=C reduction to 3-phenylpropanal under mild conditions, with Pd/TiO_2 displaying the highest activity and robust performance over several recycles. However, the Lewis acidity of TiO_2 promoted a solvent-involving side reaction in 2-propanol, with hemiacetal and ether formation, highlighting that apparent selectivity is strongly shaped by support acidity and product residence time. Rh/Al_2O_3 exhibited lower activity than Pd analogues but near-quantitative selectivity to the saturated aldehyde, whereas Rh/TiO_2 again favored hemiacetal formation. In levulinic acid hydrogenation, Pd catalysts were essentially inactive toward ketone hydrogenation even at elevated temperature and H_2 pressure, while Rh catalysts achieved high productivity with exclusive formation of γ-valerolactone, Rh/Al_2O_3 being the most active at comparatively mild pressures.

Keywords: palladium; rhodium; heterogeneous catalyst; support; hydrogenation

Academic Editor: Anker Degn Jensen

Received: 5 May 2026
Revised: 22 June 2026
Accepted: 29 June 2026
Published: 30 June 2026

1. Introduction

Heterogeneous hydrogenation catalysis plays a central role in numerous chemical industrial processes ranging from bulk petrochemicals to fine chemicals, pharmaceuticals, and sustainable transformations of biomass-derived molecules [1–5]. The performance of hydrogenation catalysts is governed not only by the nature of the active metal but also, critically, by the properties of the support, which influence metal dispersion, electronic structure, stability, and ultimately catalytic activity and selectivity [6]. Among the various classes of support, metal oxides are particularly prominent owing to their thermal and mechanical stability, high surface area, and tunable surface chemistry [6]. Consequently, oxides such as Al_2O_3, TiO_2, ZrO_2, and SiO_2 are widely employed in both academic studies

and industrial applications, either as single oxides or as mixed systems designed to exploit synergistic effects [6–14]. Alumina remains the most extensively used catalytic support because of its versatility, availability, and cost-effectiveness. In particular, γ-Al_2O_3 exhibits high porosity and surface area, together with a predominance of Lewis acidic sites that can be tailored through synthesis and treatment conditions. These features underpin its widespread use in hydrogenation catalysts, including Pd/Al_2O_3 and Rh/Al_2O_3 systems, as well as in large-scale processes such as steam reforming and Fischer–Tropsch synthesis [11]. Titanium dioxide, in its different crystalline phases, anatase and rutile, has also been extensively studied. Compared to other metal oxides, titania represents a reducible oxide support capable of strong electronic and structural interactions with supported noble metals. The phenomenon of strong metal–support interaction (SMSI), especially pronounced for noble metals supported on anatase TiO_2 after reductive treatments, can significantly modify metal accessibility, electronic properties, and resistance to sintering, thereby affecting hydrogenation performance [8,15–17]. Titania also exhibits redox properties, and its surface structure can develop Lewis acidity [6–8]. Zirconia, characterized by high thermal and chemical stability and amphoteric behavior, has attracted increasing interest due to its redox properties, particularly when doped, and its demonstrated activity in hydrogenation reactions such as CO_2 conversion [18]. Silica, typically employed in mesoporous form, offers high surface area and well-defined pore structures while remaining largely chemically inert, making it an ideal platform to isolate metal effects or to introduce tailored functionalities through surface modification. Among the most notable applications of silica-supported catalysts is MCM-41 and mesoporous SBA-15 silica; however, this material is limited by low mechanical stability under stirring conditions, which can lead to catalyst loss [9]. Within this framework, palladium and rhodium are among the most effective and widely used noble metals for hydrogenation reactions [1–5]. In heterogeneous catalysis, palladium is typically supported on oxides or activated carbon and is renowned for its high activity in the hydrogenation of C=C and C≡C bonds, and nitro, nitrile, and carbonyl functionalities as well as for dehydrogenation and isomerization reactions [10,19]. Rhodium, although less abundant and more expensive, exhibits exceptional performance in selective hydrogenations and related transformations, benefiting from its distinctive electronic properties and catalytic versatility. In heterogeneous systems, rhodium is employed in selective hydrogenations and dehydrogenations, in oxidations, and in automotive catalytic converters, together with Pt and Pd, to improve vehicle exhaust treatment systems [20,21]. Both metals, Pd and Rh, are typically dispersed as nanoparticles on oxide supports, where metal–support interactions play a decisive role in determining catalytic behavior. Despite their effectiveness, the use of Pd- and Rh-based catalysts is increasingly challenged by economic and sustainability considerations, as these metals are scarce, costly, and subject to significant market volatility. This has driven growing interest in the development of low-metal-loading catalysts that maximize atom efficiency while maintaining or even enhancing catalytic performance. High dispersion of the active phase, uniform metal distribution, and strong yet controlled metal–support interactions are key strategies to achieve this goal. In this context, mild and scalable preparation methods that avoid high-temperature calcination or activation steps are particularly attractive, as they can preserve small metal entities and reduce energy input. In the present work, we investigate the effect of different oxide supports, such as Al_2O_3, TiO_2, ZrO_2, and SiO_2, on the performance of low-loading Pd and Rh catalysts in hydrogenation reactions. By employing a simple one-pot impregnation methodology under mild conditions, developed by the authors [22–24], Pd/Al_2O_3 (Pd 0.24% *w*/*w*), Pd/TiO_2 (Pd 0.18% *w*/*w*), Pd/ZrO_2 (Pd 0.21% *w*/*w*), Pd/SiO_2 (Pd 0.37% *w*/*w*), Rh/Al_2O_3 (Rh 0.18% *w*/*w*), and Rh/TiO_2 (Rh 0.15% *w*/*w*) were prepared with the aim to elucidate how support properties such as acidity, reducibility, and metal–support interaction influence activity and selectivity. Model substrates, includ-

ing (E)-cinnamaldehyde and levulinic acid, are used to probe structure–performance relationships in hydrogenation. (E)-Cinnamaldehyde is an α,β-unsaturated aldehyde of considerable industrial relevance in fine chemicals, as its hydrogenation products constitute valuable intermediates for the manufacture of fragrances, flavors, and pharmaceutical active ingredients [25]. Cinnamaldehyde owes its reactivity to the coexistence of a carbonyl group conjugated with an olefinic double bond, and the presence of these two distinct functionalities makes cinnamaldehyde a convenient model substrate for probing catalytic activity and chemoselectivity as a function of the metal and support. Data from the literature indicate that Pd- and Rh-based catalysts typically display high activity and preferential hydrogenation of the C=C bond over the C=O bond, both kinetically and thermodynamically [25–32]. With these noble metals, adsorption and activation of the olefinic moiety are generally favored. Levulinic acid (LA) is one of the most important biomass-derived platform molecules from lignocellulosic feedstocks [33–35]. The chemical versatility of LA originates from the coexistence of carboxylic and ketone functionalities, enabling its use in esterification, redox, substitution, and polymerization reactions. As a key renewable intermediate, LA can be upgraded into a broad portfolio of value-added products relevant to the solvent, biofuel, pharmaceutical, and polymer sectors [34,35]. Among these derivatives, γ-valerolactone (GVL) is particularly attractive due to its established use as a solvent and gasoline additive, as well as its wider applicability across multiple industrial segments [36–51]. Under the temperature and acidity regimes typically employed, the most plausible pathway to GVL involves hydrogenation of the LA ketone (C=O) to the corresponding hydroxy acid, followed by intramolecular esterification (lactonization) to form the five-membered ring [52]. Efficient implementation therefore requires a bifunctional catalytic system combining metallic sites for hydrogenation with acidic sites that promote dehydration/lactonization.

2. Materials and Methods

All commercially available reagents, solvents, and chemicals were provided by Sigma Aldrich (Milan, Italy). Alumina was generously provided by Chimet (Arezzo, Italy). The catalysts and products were characterized by different analytical and spectroscopic analyses, such as GC, GC-MS, SEM, and EDX. Gas-chromatography (GC) analyses were performed on an Agilent 6850 gas chromatograph (Agilent, Santa Clara, California, USA). Gas chromatography-mass spectrometry (GC-MS) analyses were performed on a HP 5890 series II gas chromatograph interfaced to a HP 5971 quadrupole mass detector (Bangalore, India). Scanning electron microscopy (SEM) was carried out using a FE-SEM Gemini 360 ZEISS (Jena, Germany). The acceleration potential voltage was maintained at 15 keV and measurements were carried out using an In-lens detector and a Backscattered detector. Samples were deposited on conductive carbon adhesive tape and metallized by sputtering with chromium (8 nm). Elemental composition and chemical mapping were determined using a BRUKER XFlash 7 EDX detector (Milan, Italy). STEM analyses were carried out using FE-SEM Gemini 360 ZEISS (Jena, Germany), STEM module. The samples were prepared by placing one drop of catalyst dispersion on a copper grid pre-coated with a Formvar film and dried in air. Quantitative determination of palladium and rhodium in the synthesized catalysts was carried out via atomic emission spectroscopy. Analyses were performed using a microwave plasma–atomic emission spectrometer (MP-AES, Agilent Technologies 4210) (Santa Clara, California, USA), equipped with a high-temperature nitrogen plasma generated by microwave excitation.

2.1. Catalysts Preparation

2.1.1. Synthesis of TiO_2 (anatase) [53]

In a 500 mL round-bottom flask equipped with a Teflon mechanical stirrer and a bubble condenser, benzyl alcohol (201 g; 1.94 mol), acetic acid (45 g; 0.755 mol), and titanium tetraisopropoxide (53.35 g; 0.187 mol) were combined at room temperature. The mixture was heated to reflux and after 5 h, the solution became opaque and progressively increased in viscosity. The stirring rate increased, and the mixture was maintained at reflux for 24 h. The mixture was then concentrated under reduced pressure (0.5 mmHg) at approximately 70 °C until a viscous paste was obtained. The residue was treated first with ethanol and subsequently with diisopropyl ether, then filtered and dried under vacuum.

2.1.2. Pd/Al_2O_3 (Pd 0.24% *w*/*w*)

Pd/Al_2O_3 (0.24 wt%) was prepared following a one-pot procedure developed by the authors [22,23]. In a 50 mL autoclave glass liner equipped with a magnetic stir bar, $PdCl_2$ (13 mg, 0.0735 mmol), cyclopentyl methyl ether (CPME, 10 mL), trioctylamine (TOA, 110 µL, 0.252 mmol), and Al_2O_3 (2.5 g) were introduced under nitrogen atmosphere. The liner was placed in a stainless-steel autoclave under continuous nitrogen flow, which was then pressurized with H_2 (0.5 MPa). The reactor was thermostated at 25 °C using an ethylene glycol bath and stirred for 24 h. After completion, the solid was filtered under nitrogen, washed with CPME and diethyl ether, dried under vacuum, and collected.

2.1.3. Pd/TiO_2 (Pd 0.18% *w*/*w*)

$PdCl_2$ (13 mg, 0.0735 mmol), CPME (30 mL), TOA (110 µL, 0.252 mmol), and TiO_2 (2.5 g) were treated following the same procedure described for Pd/Al_2O_3 [22,23].

2.1.4. Pd/ZrO_2 (Pd 0.21% *w*/*w*)

$PdCl_2$ (13 mg, 0.0735 mmol), CPME (10 mL), TOA (110 µL, 0.252 mmol), and ZrO_2 (2.5 g) were treated following the same procedure described for Pd/Al_2O_3 [22,23].

2.1.5. Pd/SiO_2 (Pd 0.37% *w*/*w*)

$PdCl_2$ (13 mg, 0.0735 mmol), CPME (10 mL), TOA (110 µL, 0.252 mmol), and SiO_2 (2.5 g) were processed following the same protocol as for Pd/Al_2O_3 [22,23].

2.1.6. Rh/Al_2O_3 (Rh 0.18% *w*/*w*)

Rh/Al_2O_3 (0.18 wt%) was prepared following a one-pot procedure developed by the authors [22,23]. $RhCl_3 \cdot 3H_2O$ (12.5 mg, 0.0475 mmol), CPME (10 mL), TOA (110 µL, 0.252 mmol), and Al_2O_3 (2.5 g) were introduced under nitrogen into a glass liner equipped with a magnetic stir bar. The autoclave was pressurized with H_2 (0.5 MPa) and maintained at 25 °C for 24 h. The catalyst was recovered by filtration, washed with CPME and diethyl ether, dried under vacuum, and collected.

2.1.7. Rh/TiO_2 (Rh 0.15% *w*/*w*)

$RhCl_3 \cdot 3H_2O$ (12.5 mg, 0.0475 mmol), CPME (30 mL), TOA (110 µL, 0.252 mmol), and TiO_2 (2.5 g) were treated analogously to Rh/Al_2O_3 [22,23].

2.2. Hydrogenation Reactions

2.2.1. Catalytic Hydrogenation of (E)-Cinnamaldehyde (I): General Procedure

Hydrogenation reactions were conducted in a 50 mL glass liner equipped with a magnetic stir bar under a nitrogen atmosphere. Freshly distilled *(E)*-cinnamaldehyde (I) (1.9 mmol), the desired amount of catalyst, and solvent were introduced (see Tables 1–12). The liner was placed in the autoclave, which was charged with hydrogen and heated to

the desired temperature for the specified reaction time (see Tables 1–12). After completion, the autoclave was cooled to room temperature and depressurized. The mixture was centrifuged, and the supernatant was analyzed by GC and GC-MS.
GC-MS *m*/*z* (II): 134 $[M]^+$; 105 $[M\text{-}CHO]^+$; 91 $[M\text{-}C_2H_3O]^+$; 78 $[M\text{-}C_3H_4O]^+$.
GC-MS *m*/*z* (III): 136 $[M]^+$; 118 $[M\text{-}H_2O]^+$; 105 $[M\text{-}CH_2OH]^+$; 91 $[M\text{-}C_2H_5O]^+$; 77 $[M\text{-}C_3H_7O]^+$.
GC-MS *m*/*z* (IV): 178 $[M]^+$; 163 $[M\text{-}CH_3]^+$; 118 $[M\text{-}C_3H_8O]^+$; 105 $[M\text{-}C_4H_9O]^+$; 91 $[M\text{-}C_5H_3O]^+$.
GC-MS *m*/*z* (V): 194 $[M]^+$; 176 $[M\text{-}H_2O]^+$; 135 $[M\text{-}C_3H_7O]^+$; 117 $[M\text{-}C_3H_9O_2]^+$; 105 $[M\text{-}C_4H_9O_2]^+$; 91 $[M\text{-}C_5H_{11}O_2]^+$, 89 $[M\text{-}C_8H_9]^+$.

2.2.2. Catalytic Hydrogenation of Levulinic Acid (VI): General Procedure

Levulinic acid (VI) (1.1 mmol), the desired amount of catalyst, and 2-propanol were introduced into a 50 mL glass liner under nitrogen. The autoclave was charged with hydrogen and heated at the selected temperature and time (see Tables 13–16). After cooling and depressurization, the mixture was centrifuged and the supernatant analyzed by GC and GC-MS.
GC-MS *m*/*z* (VII)**:** 100 $[M]^+$; 85$[M\text{-}CH_3]^+$; 56$[M\text{-}C_2H_4O]^+$; 28$[C_2H_4]^+$.

2.2.3. Catalyst Recycling Procedure

For recycling experiments, the catalyst was recovered from the completed reaction by centrifugation (5000 rpm, 15 min). The supernatant was removed with a Pasteur pipette, and the solid catalyst was washed twice with diethyl ether, dried under vacuum, and resuspended in fresh 2-propanol containing newly added substrate and reused under identical hydrogenation conditions.

2.2.4. Catalyst Reactivation

For catalyst reactivation, the recovered catalyst was placed in an autoclave glass liner with CPME (10 mL) under nitrogen. The autoclave was pressurized with H_2 (0.5 MPa) and maintained at 25 °C for 24 h. The solid was then filtered, washed with CPME and diethyl ether, dried under vacuum, and reused.

3. Results and Discussion

3.1. Preparation and Characterisation of Pd/TiO_2 (Pd 0.18% w/w) and Rh/TiO_2 (Rh 0.15% w/w)

Pd/TiO_2 (Pd 0.18% *w*/*w*) and Rh/TiO_2 (Rh 0.15% *w*/*w*) were prepared by following a procedure developed by the authors for the preparation of the low-metal content catalysts supported on Al_2O_3 [22,23]. As shown in the SEM micrographs (Figures S1 and S2), the titania used as support exhibits a non-uniform morphology and particle size distribution, characterized by a heterogeneous distribution of grains and irregular agglomerates of varying dimensions (both coarser and finer particles). An EDX surface mapping analysis (Figure S3) shows a homogeneous distribution of palladium particles over the support. This aspect is of fundamental importance, as it ensures a high number of available active sites, which is directly correlated with high catalytic activity. SEM micrographs of Pd/TiO_2 (commercial support) and Pd/TiO_2 (homemade support) (Figures S4 and S5) highlight the presence of Pd metallic nanoparticles with dimensions between 5 and 10 nm. This was confirmed by EDX analyses (Figures S3 and S6). Also, SEM and EDX analyses of Rh/TiO_2 (Figure S7) highlight the presence of Rh nanoparticles homogeneously distributed over the support. Additional confirmation of the presence of metallic nanoparticles and their size distribution was obtained by STEM analysis, which was carried out on all catalysts. The micrographs showed the presence of both Rh and Pd nanoparticles with an average diameter of approximately 10 nm (Figures S8–S10).

3.2. Hydrogenation of (E)-Cinnamaldehyde (I)

Initially, the hydrogenation of (E)-cinnamaldehyde (I) (Scheme 1) was carried out using Pd/Al_2O_3 (Pd 0.24% *w*/*w*), and the results are reported in Table 1.

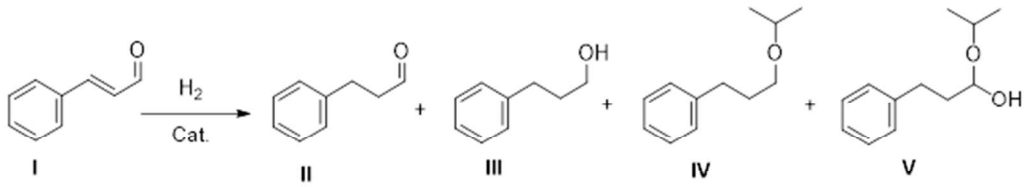

Scheme 1. Hydrogenation of (E)-cinnamaldehyde (I).

Table 1. Hydrogenation of (E)-cinnamaldehyde (I) catalyzed by Pd/Al_2O_3 (Pd 0.24% *w*/*w*).

Entry [a]	S/Pd mol	p(H_2) MPa	t (h)	Conversion (%) [b]	II Selectivity (%) [b]	III Selectivity (%) [b]	IV Selectivity (%) [b]	V Selectivity (%) [b]
1	1000/1	0.2	1	73	85	15	/	/
1r1 [c]	"	"	1	68	80	15	3	2
1r2 [c]	"	"	1	67	92	6	1	1
1r3 [c]	"	"	1	40	94	/	5	1
2	2000/1	0.2	1	34	95	5	/	/
3	2000/1	0.5	1	48	71	4	3	22
4	2000/1	1.0	1	100	70	28	1	1
4r1 [c]	"	"	1	100	74	23	1	2
4r2 [c]	"	"	1	79	87	10	1	2
5	2000/1	0.2	6	100	77	20	1	2
6	2000/1	0.1	6	100	78	15	1	6
6r1 [c]	"	"	6	100	80	12	1	7
6r2 [c]	"	"	6	100	83	14	1	2
6r3 [c]	"	"	6	51	92	6	/	2
7	5000/1	0.2	6	46	96	3	/	1
7r1	"	"	6	45	95	4	/	1
7r2	"	"	6	37	98	/	/	2
8	5000/1	0.2	22	100	83	15	/	2
8r1	"	"	22	100	82	13	1	4
8r2	"	"	22	69	90	/	1	9

[a] Reaction conditions: Substrate (I) 1.89 mmol (0.25 g); Pd/Al_2O_3 = 83.8 mg (S/Pd = 1000); Solvent: 2-propanol (6 mL); T = 40 °C. [b] Data determined by GC (%) using *n*-undecane as internal standard; [c] r = recycling experiment; " = same value as above; / = 0.

A first reaction (Entry 1), carried out at 40 °C and 0.2 MPa H_2 for 1h with a substrate-to-metal molar ratio (S/Pd) of 1000/1, afforded 73% substrate conversion, with predominant hydrogenation of the C=C bond and minor contribution from carbonyl reduction. Upon recycling (Entries 1r1–1r3), catalytic activity progressively decreased, with a pronounced drop upon the third reuse. Concomitantly, selectivity shifted toward 3-phenylpropanal (II). Formation of ether (IV) and hemiacetal (V) was also observed, consistent with the presence of Lewis-acid sites on alumina. In particular, isopropyl 3-phenylpropyl ether (IV) can form via reductive etherification between 3-phenylpropanal and 2-propanol, while the corresponding hemiacetal (V) can be generated through nucleophilic addition of 2-propanol to the aldehyde carbonyl. In both cases, interaction of 3-phenylpropanal with Lewis-acid sites on the support surface is crucial, as it facilitates alcohol addition to the carbonyl group. Noteworthy, the hemiacetal did not evolve to the acetal due to steric

constraints that hinder nucleophilic attack by a second 2-propanol molecule [25]. To reduce catalyst loading, the reaction was conducted at S/Pd = 2000/1 under identical conditions (Entry 2). Although selectivity to the saturated aldehyde (II) increased, conversion decreased to 34%, pointing to a regime limited by the number of accessible metallic sites. Increasing the hydrogen pressure to 0.5 MPa (Entry 3) conversion rose to 48% but selectivity to (II) decreased, primarily due to substantial hemiacetal (V) formation. At 1.0 MPa H_2 (Entry 4), complete conversion was achieved, yielding mainly (II) (70%) and (**III**) (28%). The consecutive C=O hydrogenation to (III) indicates that once the olefin is consumed the saturated aldehyde may remain adsorbed long enough on Pd sites to undergo further reduction. Catalyst performance was retained upon the first recycle (Entry 4r1), whereas the second recycle (Entry 4r2) exhibited reduced conversion (79%) together with a progressive increase in selectivity to (II) at the expense of (III). This trend is consistent with a decrease of accessible Pd sites probably due to sintering, poisoning, and/or mechanical losses during recovery and to a concomitant suppression of the consecutive pathway to (III), which likely requires either higher site density/metal dispersion or longer residence times on active Pd ensembles. In order to assess whether the deactivation of the recycled catalyst, in addition to potential accidental factors, could be related to structural modifications of the catalyst itself, a SEM analysis was carried out. As a matter of fact, SEM images of Pd/Al_2O_3 acquired at different magnifications, before and after use, showed that the metal nanoparticles tend to agglomerate, leading to the formation of larger particles, which can reach sizes on the order of some micrometers, thereby showing a structural modification of the catalyst induced by the reaction conditions (Figure S11). To operate under the mildest possible conditions while maintaining high conversion, reactions were always performed at 40 °C and low H_2 pressures but with extended reaction times. At S/Pd molar ratio = 2000/1 and 0.2 MPa H_2, after 6 h, conversion was complete and (II) was the predominant product (Entry 5). Halving the pressure to 0.1 MPa still afforded complete conversion (Entry 6), confirmed in the first two recycling experiments (Entries 6r1 and 6r2), whereas a sharp decrease was observed upon a further reuse (Entry 6r3). Catalyst loading was further reduced to S/Pd molar ratio = 5000/1. After 6 h (Entry 7), conversion was rather low (46%), albeit with higher selectivity to (II). Prolonging the reaction to 22 h (Entry 8) restored complete conversion, which was maintained upon the first recycle (Entry 8r1) but decreased to 69% upon the second recycle (Entry 8r2). Across these conditions, selectivity consistently favored product (II).

Cinnamaldehyde hydrogenation catalyzed by Pd/Al_2O_3 was next evaluated in different solvents under fixed conditions (40 °C, 0.2 MPa H_2, 1 h, S/Pd molar ratio = 1000/1) (Table 2).

Table 2. Hydrogenation of (E)-cinnamaldehyde (I) catalyzed by Pd/Al_2O_3 (Pd 0.24% *w*/*w*) in different solvents.

Entry [a]	Solvent	Conversion (%) [b]	II Selectivity (%) [b]	III Selectivity (%) [b]	IV Selectivity (%) [b]	V Selectivity (%) [b]
1	2-Propanol	73	85	15	/	/
1r1 [c]	"	68	80	15	3	2
1r2 [c]	"	67	92	6	1	1
1r3 [c]	"	40	94	/	5	1
2	MTBE	71	93	7	/	/
2r1 [c]	"	46	95	5	/	/
3	Isooctane	94	88	12	/	/
3r1 [c]	"	55	95	5	/	/
4	CPME	83	99	1	/	/

4r1 [c]	"	75	99	1	/	/
4r2 [c]	"	60	97	3	/	/

[a] Reaction conditions: Substrate (I) 1.89 mmol (0.25 g); (I)/Pd molar ratio = 1000/1; Pd/Al_2O_3 = 83.8 mg; Solvent: 2-propanol (6 mL); T = 40 °C; $p(H_2)$ = 0.2 MPa; t = 1 h. [b] Data determined by GC (%) using *n*-undecane as internal standard; [c] r = recycling experiment; " = same solvent as above; / = 0.

In 2-propanol, a polar protic medium in which cinnamaldehyde is readily soluble, 73% conversion was obtained with good recyclability; however, 3-phenylpropanal (II) partially reacted with the solvent to form hemiacetal (V), and the reductive etherification product (IV) was also detected (Entry 1). When non-alcoholic solvents were used, these secondary reactions were suppressed, resulting in higher selectivity to (II). In MTBE (Entry 2), conversion was comparable (71%) but decreased substantially after the first recycle. Isooctane (Entry 3) afforded high initial conversion (94%) but likewise showed marked deactivation upon recycling. Cyclopentyl methyl ether (CPME) (Entry 4) provided the most favorable compromise relative to 2-propanol, combining high selectivity to (II) (≈99%), with conversion above 83% and acceptable stability upon reuse. Nevertheless, CPME was deemed less attractive economically. Therefore, 2-propanol was selected as the solvent for subsequent hydrogenation experiments. This solvent screening shows that part of the selectivity loss observed in 2-propanol does not originate from an intrinsic shift in Pd chemoselectivity (C=C vs. C=O), but rather from competition between hydrogenation and solvent-involving transformations of the primary aldehydic product (II). Notably, apolar/ether solvents show less favorable recycling behavior, especially for MTBE and isooctane, suggesting that wetting, H_2 and substrate solubility, or poisoning phenomena can vary with the reaction medium.

Also, Pd/TiO_2 (Pd 0.18% *w*/*w*) was investigated in the hydrogenation of (E)-cinnamaldehyde (I) (Table 3).

Table 3. Hydrogenation of (E)-cinnamaldehyde (I) catalyzed by Pd/TiO_2 (Pd 0.18% *w*/*w*).

Entry [a]	S/Pd mol	T(°C)	Conversion (%) [b]	II Selectivity (%) [b]	III Selectivity (%) [b]	IV Selectivity (%) [b]	V Selectivity (%) [b]
1	1000/1	30	95	78	/	1	21
1r1 [c]	"	"	95	85	/	2	13
1r2 [c]	"	"	96	89	/	2	9
1r3 [c]	"	"	96	90	/	1	9
1r4 [c]	"	"	95	95	/	1	4
1r5 [c]	"	"	95	96	/	2	2
2	1000/1	40	100	63	/	4	33
2r1 [c]	"	"	100	76	/	1	23
2r2 [c]	"	"	100	93	/	1	6
2r3 [c]	"	"	100	92	/	1	7
2r4 [c]	"	"	100	91	/	1	8
2r5 [c]	"	"	100	94	/	1	5
3	2000/1	60	100	52	/	5	43
3r1 [c]	"	"	100	65	/	4	31
3r2 [c]	"	"	93	92	/	/	8
3r3 [c]	"	"	99	96	/	1	3
3r4 [c]	"	"	99	97	/	1	2
3r5 [c]	"	"	65	96	/	1	3
4	2000/1	40	100	66	8	6	20
4r1 [c]	"	"	100	52	6	3	39

4r2 [c]	"	"	48	90	6	3	1
5	2000/1	30	91	78	/	1	21
5r1 [c]	"	"	84	90	/	1	9
5r2 [c]	"	"	50	95	/	/	5
6	2000/1	20	37	83	/	5	12

[a] Reaction conditions: Substrate (I) 1.89 mmol (0.25 g); Pd/TiO_2 = 111.7 mg (S/Pd = 1000); t = 1h. Solvent: 2-propanol (6 mL); p(H_2) = 0.2 MPa. [b] Data determined by GC (%) using *n*-undecane as internal standard; [c] r = recycling experiment; " = same value as above; / = 0.

Under 0.2 MPa H_2 in 2-propanol, at 30 °C for 1 h and S/Pd molar ratio = 1000/1, 95% conversion was achieved with 78% selectivity to (II) (Entry 1). Owing to the Lewis acidity of TiO_2, a relevant hemiacetal (V) formation (21%) was observed, along with a minor amount of ether (IV) (1%). The catalyst exhibited excellent stability over multiple recycles (Entries 1r1–1r5), maintaining essentially constant conversion. A progressive shift in selectivity toward (II) in the recycle experiment was consistent with a gradual loss of support acidity and, consequently, reduced hemiacetal (V) formation. Increasing the temperature to 40 °C led to complete conversion (Entry 2), but selectivity to (II) decreased (63%) with increased formation of (V) (33%). Recycling experiments (Entries 2r1–2r5) confirmed sustained activity over repeated use, again accompanied by a gradual decrease in hemiacetal (V), consistent with diminishing acidity. At lower catalyst loading (S/Pd molar ratio = 2000/1), full conversion was obtained at 60 °C (Entry 3) and it was maintained for several recycles, decreasing only upon extended reuse (Entry 3r5). Temperature reduction at S/Pd molar ratio = 2000/1 revealed that complete conversion could be initially maintained at 40 °C (Entry 4), but conversion became less stable upon repeated recycling and dropped sharply at 20 °C (Entry 6). In general, increasing temperature enhanced conversion but also promoted hemiacetal (V) formation through reaction between the generated aldehyde (II) and the alcoholic solvent, as highlighted in Figure 1.

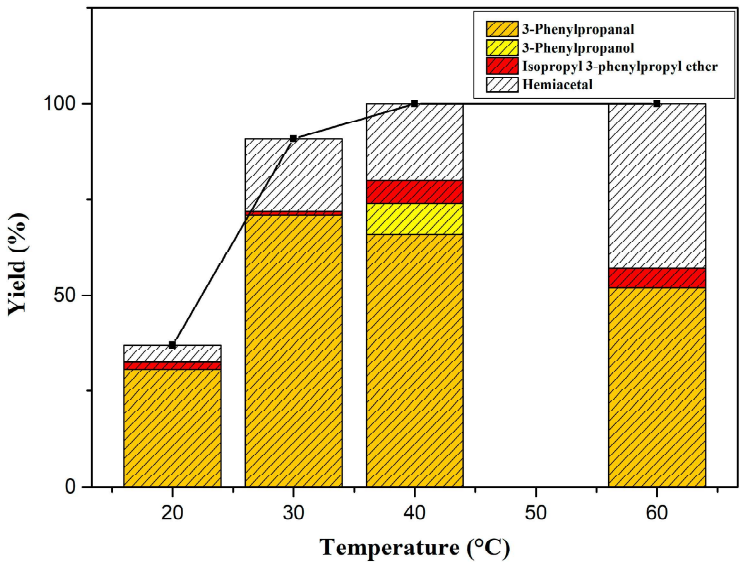

Figure 1. Temperature effect in Pd/TiO_2 (Pd 0.18% *w*/*w*) catalyzed cinnamaldehyde hydrogenation.

Due to the high activity of this catalyst, further reactions were carried out to optimize the reaction conditions, and the results are summarized in Table 4.

Table 4. Hydrogenation of (E)-cinnamaldehyde (I) catalyzed by Pd/TiO_2 (Pd 0.18% *w*/*w*) at different H_2 pressure, reaction time and S/Pd molar ratio.

Entry [a]	S/Pd Mol	p(H_2) MPa	t (h)	Conversion (%) [b]	II Selectivity (%) [b]	III Selectivity (%) [b]	IV Selectivity (%) [b]	V Selectivity (%) [b]
1	2000/1	0.1	1	100	56	4	4	36
1r1 [c]	"	"	"	100	65	6	3	26
1r2 [c]	"	"	"	60	81	/	3	16
2	5000/1	0.2	1	93	80	/	2	18
2r1 [c]	"	"	"	78	88	/	2	10
2r2 [c]	"	"	"	20	93	/	1	6
3	5000/1	0.2	3	100	34	10	4	52
3r1 [c]	"	"	"	74	70	/	3	27
3r2 [c]	"	"	"	27	90	/	6	4

[a] Reaction conditions: Substrate (I) 1.89 mmol (0.25 g); Pd/TiO_2 = 55.9 mg (S/Pd = 2000); Solvent: 2-propanol (6 mL); T = 40 °C. [b] Data determined by GC (%) using *n*-undecane as internal standard; [c] r = recycling experiment; " = same value as above; / = 0.

At 40 °C and S/Pd molar ratio = 2000/1, lowering H_2 pressure to 0.1 MPa still afforded full conversion with the fresh catalyst and in the first recycle (Entry 1 and 1r1), but conversion decreased substantially upon a second recycle (Entry 1r2). At S/Pd mola ratio = 5000/1 and 0.2 MPa H_2, conversion remained high but incomplete after 1 h and no alcohol (III) was detected (Entry 2), indicating preferential C=C hydrogenation. Extending the reaction time to 3 h (Entry 3) restored full conversion but shifted selectivity strongly toward hemiacetal (V), highlighting the combined influence of TiO_2 acidity and prolonged reaction time of aldehyde (II) with 2-propanol. In recycling tests performed at the high S/Pd molar ratio = 5000/1, rapid loss of activity was observed, plausibly attributable to accidental catalyst deactivation (e.g., oxygen exposure/poisoning) and/or catalyst loss during recovery (Entry 3r1 and 3r2); under low-metal conditions, even minor mass losses can significantly impact conversion.

Similarly to the Pd/Al_2O_3 catalyst, the catalytic activity of Pd/TiO_2 was also evaluated in different solvents. The results are summarized in Table 5.

Table 5. Hydrogenation of (E)-cinnamaldehyde (I) catalyzed by Pd/TiO_2 (Pd 0.18% *w*/*w*) in different solvents.

Entry [a]	Solvent	Conversion (%) [b]	II Selectivity (%) [b]	III Selectivity (%) [b]	IV Selectivity (%) [b]	V Selectivity (%) [b]
1	2-Propanol	93	80	/	2	18
2	MTBE	9	100	/	/	/
3	Isooctane	3	100	/	/	/
4	CPME	16	100	/	/	/

[a] Reaction conditions: Substrate (I) 1.89 mmol (0.25 g); (I)/Pd molar ratio = 5000/1; Pd/TiO_2 = 22.3 mg; Solvent (6 mL); T= 40 °C; p(H_2) = 0.2 MPa; t= 1 h. [b] Data determined by GC (%) using *n*-undecane as internal standard; / = 0.

Under fixed conditions (40 °C, 0.2 MPa H_2, 1 h, S/Pd molar ratio = 5000/1), 2-propanol afforded markedly higher conversion than MTBE, isooctane, or CPME. Although non-alcoholic solvents provided quantitative selectivity to (II) (Entries 2–4), conversions were very low, whereas 2-propanol enabled higher conversion at the expense of side reactions (formation of ether (IV) and hemiacetal (V)) (Entry 1).

For comparison, hydrogenation tests of cinnamaldehyde (I) were also carried out using Pd/TiO_2 (Pd 0.18% *w*/*w*), obtained by employing TiO_2 synthesized in-house according to a literature-reported procedure [53] that yields pure anatase rather than an anatase–rutile mixture, as in the commercial TiO_2 previously used. The results are described in Table 6.

Table 6. Hydrogenation of (E)-cinnamaldehyde (I) catalyzed by Pd/TiO_2 (Pd 0.18% *w*/*w*) (TiO_2 = anatase).

Entry [a]	S/Pd mol	T (°C)	P(H_2) MPa	t (h)	Conversion (%) [b]	II Selectivity (%) [b]	III Selectivity (%) [b]	IV Selectivity (%) [b]	V Selectivity (%) [b]
1	1000	30	0.2	1	100	37	63	/	/
1r1 [c]	"	"	"	"	74	43	56	1	/
2	2000	"	"	"	30	41	56	/	3
3	"	"	"	3	72	42	55	3	/
3r1 [c]	"	"	"	"	65	49	51	/	/
4	"	30	0.5	1	51	41	59	/	/
5	"	"	1.0	1	54	40	56	4	/
6	"	40	0.5	1	87	49	51	/	/
6r1 [c]	"	"	"	"	52	46	42	11	/
7	"	"	"	3	100	42	55	3	/
7r1 [c]	"	"	"	"	96	52	41	5	2
7r2 [c]	"	"	"	"	85	47	48	4	1

[a] Reaction conditions: Substrate (I) 1.89 mmol (0.25 g); Pd/TiO_2 = 55.9 mg (S/Pd = 2000); Solvent: 2-propanol (6 mL). [b] Data determined by GC (%) using *n*-undecane as internal standard; [c] r = recycling experiment; " = same value as above; / = 0.

At S/Pd = 1000 (Entry 1), complete conversion is achieved after 1 h at 30 °C and 0.2 MPa H_2, with products (II) and (III) formed in 37% and 63% selectivity, respectively. In a recycle experiment (Entry 1r1), conversion decreases to 74%, while the selectivity pattern remains comparable (II 43%, III 56%), with only traces of (IV) (1%). Increasing the substrate-to-metal ratio to S/Pd = 2000 (Entry 2) under the same temperature, pressure, and time (30 °C, 0.2 MPa, 1 h) leads to a marked decrease in conversion (30%), indicating that catalyst productivity becomes limiting at higher substrate loading. Nevertheless, the selectivity toward (III) (56%) remains essentially unchanged compared to Entry 1, suggesting that intrinsic chemoselectivity is not significantly affected by S/Pd ratio at low conversion. Extending the reaction time to 3 h at S/Pd = 2000 (Entry 3) increases conversion to 72%, with selectivity still dominated by (III) (55%) and (II) (42%), and minor formation of (IV) (3%). Entry 3r1 (same conditions) gives slightly lower conversion (65%) and a nearly equimolar distribution of (II) (49%) and (III) (51%), again indicating modest variability but an overall stable selectivity profile. The effect of hydrogen pressure was evaluated at S/Pd = 2000 and 30 °C. Increasing pressure from 0.2 MPa (entry 2) to 0.5 MPa (Entry 4) improves conversion from 30% to 51% after 1 h, while further increasing to 1.0 Mpa (Entry 5) does not provide additional benefits (54% conversion). This suggests that hydrogen availability enhances reaction rate up to a certain threshold, beyond which mass-transfer or adsorption phenomena may limit further rate enhancement. Importantly, selectivity toward (III) (56–59%) remains largely unaffected by pressure, indicating that the relative hydrogenation pathways are not strongly pressure-dependent within this range. Temperature has a more pronounced impact. At 40 °C and 0.5 MPa H_2 (Entry 6), conversion rises sharply to 87% after 1 h, compared to 51% at 30 °C (Entry 4), demonstrating a clear kinetic acceleration. Notably, selectivity shifts toward a more balanced distribution between (II) (49%)

and (III) (51%). However, in the replicate experiment (Entry 6r1), conversion drops to 52% and a significant amount of (IV) (11%) appears, accompanied by a decrease in (III) (42%). This may indicate that at higher temperatures, secondary hydrogenation pathways becomes more competitive, leading to deeper hydrogenation (IV). Prolonging the reaction to 3 h (Entry 7) results in complete conversion, with selectivity again favoring (III) (55%) over (II) (42%), and minor (IV) formation (3%). The catalytic data reported in Table 3 and Table 6 reveal significant differences in activity and, above all, in chemoselectivity of Pd/TiO_2 (0.18% *w*/*w*) in the hydrogenation of (E)-cinnamaldehyde (I), highlighting the strong influence of reaction conditions and, likely, catalyst/support features. For, instance, in Table 3 (Entry 1), at S/Pd = 1000 and 30 °C for 1 h, conversion is high (95–96%) and the reaction is markedly selective toward product (II) (78–96%), while product (V) accounts for 2–21% and (IV) is formed only in traces (1–2%). Product (III) is not detected. In contrast, under comparable temperature and S/Pd conditions in Table 6 (Entry 1, 0.2 MPa H_2), complete conversion (100%) is achieved, but the selectivity pattern is dramatically different: product (III) is the major product (63%), while (II) accounts for only 37%, and (V) is absent. Thus, although both systems are highly active, the data of Table 3 shows a strong preference for formation of (II), whereas those of Table 6 clearly favors (III). This indicates a substantial change in hydrogenation pathway selectivity, likely related to differences in the physicochemical properties of the TiO_2 support. In all cases, in Table 3, product (V) is consistently observed (up to 43% in entry 3), particularly at higher temperature and S/Pd, while (IV) is generally a minor product (≤6%). Importantly, (III) is essentially absent except in Entry 4 (S/Pd = 2000, 40 °C), where it appears in low selectivity (6–8%). In Table 6, product (V) is minor or absent, whereas (III) is systematically formed in significant amounts (≈50–63%). Product (IV) appears only under more forcing conditions (higher temperature or longer time), indicating secondary hydrogenation pathways. The comparison highlights two markedly different catalytic behaviors:

Table 3: high chemoselectivity toward (II) over a wide range of S/Pd and temperature, even at full conversion, with (V) as the main secondary product and almost no formation of (III).

Table 6: predominant formation of (III), with (II) as co-product and only minor amounts of (IV) and (V), and selectivity relatively insensitive to pressure changes.

These differences strongly suggest that the catalytic surface properties differ between the two series of experiments. Possible factors include differences in TiO_2 phase composition (pure anatase vs. anatase/rutile mixture), metal dispersion or metal–support interactions, and hydrogen adsorption/activation capacity under different pressures.

Finally, two new catalytic systems, namely Pd/ZrO_2 (Pd 0.21% *w*/*w*) and Pd/SiO_2 (Pd 0.37% *w*/*w*), were tested in the hydrogenation of (E)-cinnamaldehyde (I), and the results are reported in Table 7.

Table 7. Hydrogenation of (E)-cinnamaldehyde (**I**) catalyzed by Pd/ZrO_2 (Pd 0.21% *w*/*w*) and by Pd/SiO_2 (Pd 0.37% *w*/*w*).

Entry [a]	Catalyst	S/Pd mol	t (h)	Conversion (%) [b]	II Selectivity (%) [b]	III Selectivity (%) [b]	IV Selectivity (%) [b]	V Selectivity (%) [b]
1	Pd/ZrO_2	1000/1	1	18	96	/	4	/
2	"	2000/1	1	13	87	/	10	3
3	"	2000/1	6	56	90	/	7	3
4	"	2000/1	22	100	67	32	/	1
4r1 [c]	"	"	"	84	78	12	/	10
4r2 [c]	"	"	"	50	92	/	3	5

5	Pd/SiO_2	1000/1	1	33	100	/	/	/
6	"	2000/1	1	17	93	/	5	2
7	"	2000/1	6	41	100	/	/	/
8	"	2000/1	22	100	85	13	/	2
8r1 [c]	"	"	"	46	96	/	/	4

[a] Reaction conditions: Substrate (I) 1.89 mmol (0.25 g); Pd/ZrO_2 = 95.8 mg (S/Pd = 1000); Pd/SiO_2 = 54.3 mg (S/Pd = 1000); Solvent: 2-propanol (6 mL); T = 40 °C; $p(H_2)$ = 0.2 MPa. [b] Data determined by GC (%) using *n*-undecane as internal standard; [c] r = recycling experiment; " = same catalyst as above; / = 0.

Pd/ZrO_2 (Pd 0.21% *w*/*w*) exhibited low activity at short reaction times under the examined conditions (40 °C, 0.2 MPa H_2), albeit with high selectivity to (II) (Entries 1–3). Increasing reaction time to 22 h afforded full conversion but lowered selectivity due to subsequent carbonyl reduction to (III) (Entry 4). Catalyst recycling led to substantial activity losses (Entry 4r1 and 4r2). Given its inferior activity relative to Pd/Al_2O_3 and Pd/TiO_2, Pd/ZrO_2 was not further investigated. Similarly, Pd/SiO_2 (Pd 0.37% *w*/*w*) required long reaction times to achieve full conversion (Entry 8). While selectivity to (II) was generally higher than with Pd/ZrO_2 under comparable long-time conditions, consistent with the more neutral character of silica compared with zirconia, overall activity remained lower than that of Pd/Al_2O_3 and Pd/TiO_2, and further studies were not pursued. For both catalysts, the increased consecutive hydrogenation to (III) is consistent with increased contact time between product and catalyst. The contrast between supports further suggests that the greater acidity of zirconia may favor additional pathways, whereas silica, generally considered more neutral, better preserves selectivity to (II) despite remaining comparatively sluggish. Among Pd catalysts, Pd/TiO_2 (0.18% Pd *w*/*w*) is the most active: 95% conversion is achieved already at 30 °C (0.2 MPa, 1 h) and quantitative conversion at 40 °C (Table 4). This superior performance relative to Al_2O_3, SiO_2, and ZrO_2 is consistent with higher Pd dispersion and/or beneficial metal–support interactions that facilitate hydrogen activation and C=C hydrogenation. However, the pronounced Lewis acidity of TiO_2 strongly enhances hemiacetal formation (V), which can reach substantial levels (up to 33–43% under several conditions; Table 4) and may even become the dominant product at longer times and low metal loading. The temperature dependence (Figure 1) further indicates that increases in conversion are accompanied by increased (V), highlighting that optimization cannot rely solely on maximizing substrate conversion; instead, it must minimize the residence time of (II) in an acidic environment in the presence of an alcoholic solvent.

At this stage, it was of interest to evaluate the activity of our catalysts in comparison with selected commercially available ones, such as Pd/Al_2O_3 (Pd 2% *w*/*w*) and Pd/C (Pd 5% *w*/*w*) (Table 8).

Table 8. Catalytic performance of synthesized and commercial supported Pd catalysts in the hydrogenation of (E)-cinnamaldehyde (I).

Entry [a]	Catalyst	Conversion (%) [b]	II Selectivity (%) [b]	III Selectivity (%) [b]	IV Selectivity (%) [b]	V Selectivity (%) [b]
1	Pd/ZrO_2 (0.21%)	18	96	/	4	/
2	Pd/SiO_2 (0.37%)	33	100	/	/	/
3	Pd/TiO_2 (0.18%)	100	63	/	4	33
3r1 [c]	"	100	76	/	1	23
3r2 [c]	"	100	93	/	1	6
3r3 [c]	"	100	92	/	1	7

7	Pd/Al_2O_3 (0.24%)	73	85	15	/	/
7r1 [c]	"	68	80	15	3	2
7r2 [c]	"	67	92	6	1	1
7r3 [c]	"	40	94	/	5	1
8	Pd/Al_2O_3 (2%)	72	100	/	/	/
8r1 [c]	"	66	99	/	/	1
8r2 [c]	"	62	100	/	/	/
8r3 [c]	"	38	100	/	/	/
9	Pd/C (5%)	100	62	14	3	21
9r1 [c]	"	100	73	20	1	6
9r2 [c]	"	90	73	4	1	22
9r3 [c]	"	79	76	1	1	22

[a] Reaction conditions: Substrate (I) 1.89 mmol (0.25 g); (I)/Pd molar ratio = 1000/1; Solvent: 2-propanol (6 mL); T = 40 °C; $p(H_2)$ = 0.2 MPa; t = 1h. [b] Data determined by GC (%) using *n*-undecane as internal standard; [c] r = recycling experiment; " = same catalyst as above; / = 0.

Hydrogenation tests were also carried out using commercially available heterogeneous Pd catalysts and compared with our synthesized systems under identical conditions (40 °C, 0.2 MPa H_2, 1 h, S/Pd molar ratio = 1000/1) (Table 8 and Figure 2). Pd/ZrO_2 and Pd/SiO_2 were highly selective to 3-phenylpropanal (II) but exhibited limited activity, whereas Pd/Al_2O_3 and Pd/TiO_2 were the most effective among the synthesized catalysts. Pd/Al_2O_3 (Pd 0.24% *w*/*w*) displayed activity comparable to commercial Pd/Al_2O_3 (Pd 2% *w*/*w*), but the commercial catalyst was more selective to (II) (100% vs. 85% in the first run), suggesting that the commercial material may combine more favorable Pd dispersion and/or a reduced tendency for consecutive carbonyl hydrogenation (and/or reduced influence of acidic sites on product transformation). Pd/TiO_2 (Pd 0.18% *w*/*w*) emerged as the best-performing catalyst overall, providing complete conversion maintained across multiple recycles; it therefore exhibited higher activity than both the synthesized and commercial catalysts tested. Among commercial materials, Pd/C (Pd 5% *w*/*w*) performed best, yet it showed activity losses from the second recycle onward and generally lower selectivity relative to Pd/TiO_2.

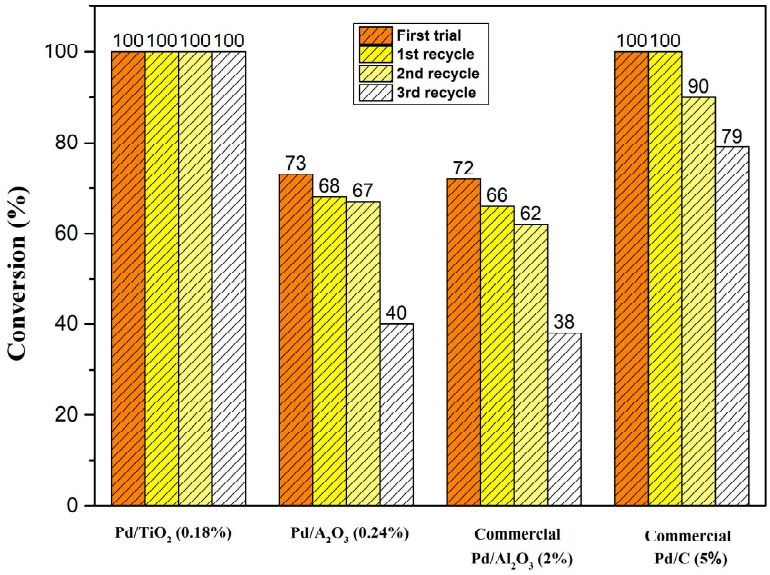

Figure 2. Comparison of catalytic performance of synthesized and commercial supported Pd catalysts in the hydrogenation of (E)-cinnamaldehyde (I).

To benchmark Pd-based systems, two Rh catalysts, namely Rh/Al_2O_3 (Rh 0.18% *w*/*w*) and Rh/TiO_2 (Rh 0.15% *w*/*w*), were evaluated (Tables 9 and 10).

Table 9. Hydrogenation of (E)-cinnamaldehyde (I) catalyzed by Rh/Al_2O_3 (Rh 0.18% *w*/*w*).

Entry [a]	S/Rh mol	p(H_2) MPa	t (h)	Conversion (%) [b]	II Selectivity (%) [b]	III Selectivity (%) [b]	IV Selectivity (%) [b]	V Selectivity (%) [b]
1	2000/1	0.2	1	6	100	/	/	/
2	2000/1	0.2	22	26	99	/	/	1
3	1000/1	0.2	1	37	100	/	/	/
4	1000/1	0.2	6	71	100	/	/	/
5	1000/1	0.2	22	100	100	/	/	/
5r1 [c]	"	"	"	100	99	/	/	1
5r2 [c]	"	"	"	41	98	/	/	2
6	1000/1	0.5	6	82	100	/	/	/
6r1 [c]	"	"	"	57	99	/	/	1
7	1000/1	1.0	6	100	100	/	/	/
7r1 [c]	"	"	"	83	99	/	/	1

[a] Reaction conditions: Substrate (I) 1.89 mmol (0.25 g); Rh/Al_2O_3 = 108 mg (S/Rh = 1000); Solvent: 2-propanol (6 mL); T = 40 °C. [b] Data determined by GC (%) using *n*-undecane as internal standard; [c] r = recycling experiment; " = same value as above; / = 0.

As shown in Table 9, Rh/Al_2O_3 was essentially chemoselective for C=C hydrogenation, yielding (II) with negligible formation of hemiacetal (V) (≤2%) and no detectable (III) or etherification product (IV) under the conditions tested. However, compared with Pd catalysts, Rh/Al_2O_3 was substantially less active. At S/Rh molar ratio = 2000/1, conversion was only 6% after 1 h (Entry 1) and remained low (26%) even after 22 h (Entry 2). Increasing catalyst loading to S/Rh molar ratio = 1000/1 improved conversion to 37% (1 h) (Entry 3) and 71% (6 h) (Entry 4), reaching full conversion only after 22 h (Entry 5). The catalyst retained performance upon one recycle, while activity decreased upon further reuse, suggesting that Rh sites may be more susceptible to poisoning/oxidation or that catalyst recovery losses become disproportionately impactful. Similarly to the approach adopted for Pd/Al_2O_3, the recycled rhodium-based catalyst was also examined to determine whether it had undergone structural changes that could account for the observed decrease in catalytic activity. As a matter of fact, TEM images reveal a significant structural evolution before and after use. Initially, the catalyst exhibits a nanostructured morphology, with rhodium nanoparticles ranging in size from 8 to 13 nm (Figure S12). However, TEM analysis of the recycled catalyst shows a marked increase in particle size, with rhodium particles reaching dimensions between 19 and 29 nm (Figure S12). This increase in particle size suggests the occurrence of particle agglomeration and/or sintering during the catalytic process, thereby resulting in altered catalytic activity. At 6 h reaction time, increasing H_2 pressure from 0.2 to 0.5 MPa increased conversion to 82% (Entry 6). A further increase of pressure to 1.0 MPa afforded complete conversion (Entry 7). Recycling experiments showed activity loss but maintained near-quantitative selectivity to (II). Overall, Rh/Al_2O_3 was less active than Pd analogues but markedly more selective to (II), with negligible hemiacetal (V) formation.

By comparison, Rh/TiO_2 was also tested in the hydrogenation of (E)-cinnamaldehyde (I) (Table 10). Under conditions comparable to those used for Rh/Al_2O_3 (S/Rh molar ratio = 1000/1, 40 °C, 0.2 MPa H_2, 6 h), Rh/TiO_2 exhibited inferior conversion and selectivity, affording 40% conversion and appreciable hemiacetal (V) formation (23%), consistent with TiO_2 acidity (Entry 1). Extending the reaction to 22 h increased conversion to 77%

(Entry 2) and maintained it over two recycles before a sharp decline upon further reuse (Entries 2r1–2r3). Increasing H_2 pressure to 1.0 MPa provided only a modest conversion gain but strongly increased (V) selectivity (75%). At 2.0 MPa, full conversion was achieved, but selectivity remained poor with (II) and (V) formed in comparable amounts (Entry 4).

Table 10. Hydrogenation of (E)-cinnamaldehyde (I) catalyzed by Rh/TiO_2 (Rh 0.15% *w*/*w*).

Entry [a]	p(H_2) MPa	t (h)	Conversion (%) [b]	II Selectivity (%) [b]	III Selectivity (%) [b]	IV Selectivity (%) [b]	V Selectivity (%) [b]
1	0.2	6	40	76	/	1	23
2	0.2	22	77	70	/	3	27
2r1 [c]	"	"	77	72	/	1	27
2r2 [c]	"	"	77	78	/	1	21
2r3 [c]	"	"	22	74	/	2	23
3	1.0	22	81	19	/	6	75
3r1 [c]	"	"	72	26	/	7	67
3r2 [c]	"	"	16	51	/	5	44
4	2.0	22	100	48	/	3	49
4r1 [c]	"	"	80	44	/	5	51
4r2 [c]	"	"	25	46	/	4	50

[a] Reaction conditions: Substrate (I) 1.89 mmol (0.25 g); Substrate/Rh molar ratio = 1000/1; Rh/TiO_2 = 129.6 mg; Solvent: 2-propanol (6 mL); T = 40 °C. [b] Data determined by GC (%) using *n*-undecane as internal standard; [c] r = recycling experiment; " = same value as above; / = 0.

At this point, it was interesting to examine the influence of temperature while keeping the other reaction parameters constant. Temperature effects at 1.0 MPa H_2 for 6 h, with S/Rh molar ratio = 1000/1 (Table 11, Figure 3), showed that conversion increased with temperature, reaching 100% at 80 °C (Entry 4); however, selectivity shifted strongly toward hemiacetal (V) at ≥60 °C (Entries 3 and 4). This behavior can be rationalized by a dominant kinetic contribution: although higher temperature would thermodynamically favor hemiacetal dissociation, the rate of hemiacetal formation increases sufficiently to yield higher observed (V) selectivity. Increased temperature also enhanced formation of ether (IV).

Table 11. Hydrogenation of (E)-cinnamaldehyde (I) catalyzed by Rh/TiO_2 (Rh 0.15% *w*/*w*) at different temperatures.

Entry [a]	T (°C)	Conversion (%) [b]	II Selectivity (%) [b]	III Selectivity (%) [b]	IV Selectivity (%) [b]	V Selectivity (%) [b]
1	20	64	90	/	/	10
2	40	70	66	9	1	24
3	60	70	12	/	5	83
4	80	100	7	/	8	85

[a] Reaction conditions: Substrate (I) 1.89 mmol (0.25 g); Substrate/Rh molar ratio = 1000/1; Rh/TiO_2 = 129.6 mg; Solvent: 2-propanol (6 mL); p(H_2) = 1.0 MPa; t = 6 h. [b] Data determined by GC (%) using *n*-undecane as internal standard; / = 0.

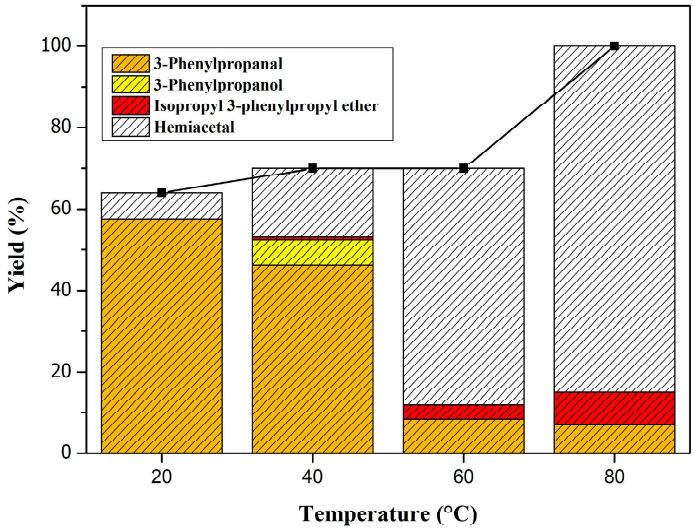

Figure 3. Temperature influence in the hydrogenation of (E)-cinnamaldehyde (I) catalyzed by Rh/TiO_2 (Rh 0.15% *w*/*w*).

Hydrogenation tests were also conducted with commercially available Rh catalysts (Table 12, Figure 4). A comparison of Rh catalysts further indicated that synthesized Rh/Al_2O_3 outperformed Rh/TiO_2 in both conversion and selectivity under the selected conditions (40 °C, 0.2 MPa H_2, 6 h), with the latter producing substantial hemiacetal (V) due to TiO_2 acidity. Both synthesized Rh catalysts were more active than commercial Rh/Al_2O_3 (5 wt%) and Rh/C (5 wt%), plausibly reflecting improved dispersion of the active phase arising from the synthesis method and/or support choice. Commercial Rh/Al_2O_3 (Entry 3) also showed lower selectivity than the synthesized analogue, consistent with concurrent, albeit limited, C=O hydrogenation. The commercial Rh/C catalyst exhibited the poorest performance, with low conversion and predominant hemiacetal (V) formation (Entry 4).

Table 12. Catalytic performance of synthesized and commercial supported Rh catalysts in the hydrogenation of (E)-cinnamaldehyde (I).

Entry [a]	Catalyst	Conversion (%) [b]	II Selectivity (%) [b]	III Selectivity (%) [b]	IV Selectivity (%) [b]	V Selectivity (%) [b]
1	Rh/Al_2O_3 (0.18%)	71	100	/	/	/
2	Rh/TiO_2 (0.15%)	40	76	/	1	23
3	Rh/Al_2O_3 (5%)	25	93	7	/	/
4	Rh/C (5%)	13	36	/	/	64

[a] Reaction conditions: Substrate (I) 1.89 mmol (0.25 g); Substrate/Rh molar ratio = 1000/1; Solvent: 2-propanol (6 mL); T = 40 °C; $p(H_2)$ = 0.2 MPa; t = 6 h. [b] Data determined by GC (%) using *n*-undecane as internal standard; / = 0.

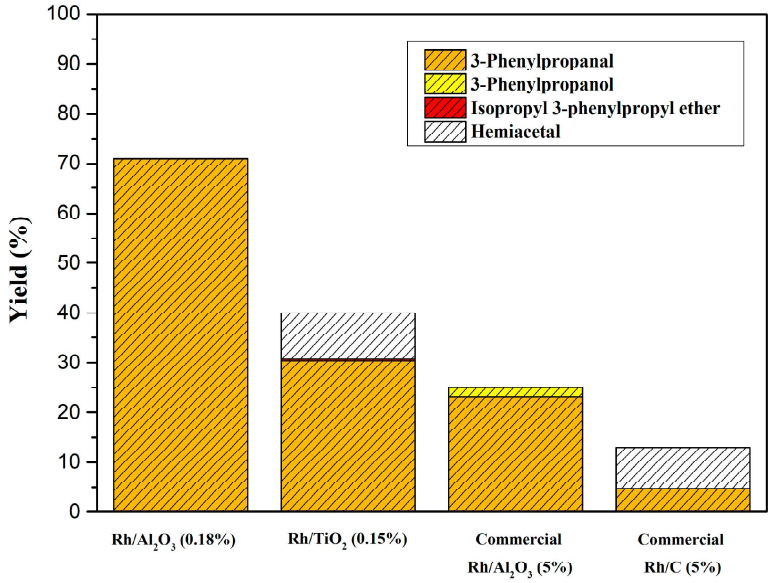

Figure 4. Comparison of catalytic performance of synthesized and commercial supported Rh catalysts in the hydrogenation of (E)-cinnamaldehyde (I).

3.3 Hydrogenation of Levulinic Acid (VI)

As in the case of (E)-cinnamaldehyde (I), the hydrogenation of levulinic acid (VI) (Scheme 2) was initially carried out using palladium-based catalysts. The results are reported in Table 13.

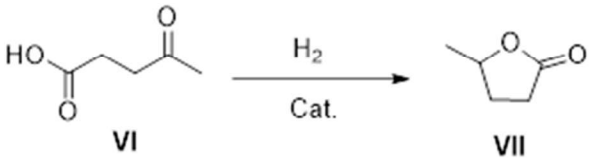

Scheme 2. Hydrogenation of levulinic acid (VI).3.3

Table 13. Hydrogenation of levulinic acid (VI) catalyzed by Pd/Al_2O_3 (Pd 0.24% *w*/*w*) and Pd/TiO_2 (Pd 0.18% *w*/*w*).

Entry [a]	Catalyst	S/Pd Moli	t(h)	Conversion (%) [b]	VII Selectivity (%) [b]
1	Pd/Al_2O_3 (0.24%)	500/1	6	7	100
2	"	500/1	22	8	100
3	"	1000/1	22	6	100
4	Pd/TiO_2 (0.18%)	500/1	6	7	100
5	"	500/1	22	8	100
6	"	1000/1	22	4	100

[a] Reaction conditions: Substrate (VI) 1.07 mmol (0.125 g); Pd/Al_2O_3 = 47.4 mg (S/Pd = 1000); Pd/TiO_2 = 63.2 mg (S/Pd = 1000); Solvent: 2-propanol (6 mL); T = 80 °C; $p(H_2)$ = 2.0 MPa. [b] Data determined by GC (%) using *n*-undecane as internal standard; " = same catalyst as above.

Levulinic acid (VI) hydrogenation catalyzed by Pd/Al_2O_3 and Pd/TiO_2 was evaluated at substrate-to-metal molar ratios (S/Pd) of 500/1 and 1000/1, respectively, at 80 °C and 2.0 MPa H_2 for 6 or 22 h (Table 13). As expected, under all conditions examined, both Pd catalysts exhibited very low activity toward hydrogenation of the ketone functionality,

affording conversions in the 4–8% range despite the comparatively forcing reaction conditions.

Better results were obtained in the presence of Rh/Al_2O_3 (Table 14). The hydrogenation of levulinic acid (VI) was performed under more demanding conditions than those used for cinnamaldehyde (I). The reference experiment (Entry 1) was carried out at S/Rh molar ratio = 500/1, 80 °C, and 2.0 MPa H_2 for 6 h. Under these conditions, (VI) was converted nearly quantitatively (99%) to γ-valerolactone (VII), which was the sole detectable product (100% selectivity). Catalyst activity remained high through the third recycle (Entries 1r1–1r3), followed by a more pronounced decline upon the fourth reuse (Entry 1r4). The effect of hydrogen pressure was subsequently examined by stepwise reduction while maintaining the other parameters constant. At 1.0 MPa (Entry 2) and 0.5 MPa (Entry 3), conversion remained essentially quantitative (98–99%) with complete selectivity to (VII). Lowering the temperature to 60 °C at 0.5 MPa (Entry 4), conversion decreased to 86%, indicating that temperature becomes limiting under reduced-pressure operation. Further decreasing H_2 pressure to 0.2 MPa (Entry 5) led to 78% conversion after 6 h at 80 °C. Extending the reaction time to 22 h at 0.2 MPa (Entry 6) restored near-complete conversion (99%), and high activity was maintained for two recycling runs (Entries 6r1 and 6r2), before a sharp drop in conversion (44%) at the third recycle (Entry 6r3). Notably, selectivity to (VII) remained quantitative throughout all Rh/Al_2O_3 catalyzed experiments.

Table 14. Hydrogenation of levulinic acid (VI) catalyzed by Rh/Al_2O_3 (Rh 0.18% *w*/*w*).

Entry [a]	T (°C)	p(H_2) MPa	t (h)	Conversion (%) [b]	VII Selectivity (%) [b]
1	80	2.0	6	99	100
1r1 [c]	"	"	"	92	100
1r2 [c]	"	"	"	88	100
1r3 [c]	"	"	"	87	100
1r4 [c]	"	"	"	65	100
2	80	1.0	6	98	100
2r1 [c]	"	"	"	98	100
2r2 [c]	"	"	"	77	100
2r3 [c]	"	"	"	55	100
3	80	0.5	6	99	100
3r1 [c]	"	"	"	80	100
3r2 [c]	"	"	"	64	100
4	60	0.5	6	86	100
4r1 [c]	"	"	"	52	100
5	80	0.2	6	78	100
5r1 [c]	"	"	"	36	100
6	80	0.2	22	99	100
6r1 [c]	"	"	"	100	100
6r2 [c]	"	"	"	93	100
6r3 [c]	"	"	"	44	100

[a] Reaction conditions: Substrate (VI) 1.07 mmol (0.125 g); (VI)/Rh molar ratio = 500/1; Rh/Al_2O_3 = 122.3 mg; Solvent: 2-propanol (6 mL). [b] Data determined by GC (%) using *n*-undecane as internal standard; [c] r = recycling experiment; " = same value as above.

Also, Rh/TiO_2 was employed as a catalyst in the hydrogenation of levulinic acid (VI), and the results are reported in Table 15. Under conditions analogous to those employed for Rh/Al_2O_3 (S/Rh molar ratio = 500/1, 0.2 MPa H_2, 6 h), Rh/TiO_2 was poorly active (21% conversion) but fully selective to (VII) (Entry 1). Increasing H_2 pressure to 1.0 MPa (Entry 2) improved conversion to 56%, and further pressure increasing to 2.0 MPa (Entry 3) af-

forded quantitative conversion (100%), again with exclusive formation of (VII). However, a substantial loss of activity emerged upon recycling, with conversion decreasing by approximately half from the second reuse onward (Entries 2r2, 3r2, and 3r3), indicating limited stability under repeated operation. Reducing catalyst loading to S/Rh molar ratio = 1000/1 at 2.0 MPa H_2 lowered conversion to 35% after 6 h (Entry 4). Extending the reaction time to 22 h (Entry 5) restored complete conversion (100%), yet recycling again resulted in severe deactivation (45% conversion) (Entry 5r1). In all experiments, selectivity remained quantitative to (VII). The results obtained suggest that, on TiO_2, either the rate of carbonyl reduction or the effective availability of activated hydrogen on Rh is more constrained than on Al_2O_3, thereby requiring a higher driving force in terms of hydrogen pressure to sustain high turnover. The activity loss during recycles is consistent with a combination of lower dispersion and/or reduced stability of Rh on TiO_2 relative to Al_2O_3, greater susceptibility of the support surface to modification in a protic medium, and a larger impact of handling-related losses when the system already operates at moderate pressures.

Table 15. Hydrogenation of levulinic acid (VI) catalyzed by Rh/TiO_2 (Rh 0.15% *w*/*w*).

Entry [a]	S/Rh mol	p(H_2) MPa	t (h)	Conversion (%) [b]	VII Selectivity (%) [b]
1	500/1	0.2	6	21	100
2	500/1	1.0	6	56	100
2r1 [c]	"	"	"	49	100
2r2 [c]	"	"	"	22	100
3	500/1	2.0	6	100	100
3r1 [c]	"	"	"	94	100
3r2 [c]	"	"	"	54	100
3r3 [c]	"	"	"	34	100
4	1000/1	2.0	6	35	100
5	1000/1	2.0	22	100	100
5r1 [c]	"	"	"	45	100

[a] Reaction conditions: Substrate (VI) 1.07 mmol (0.125 g); Rh/TiO_2 = 73.4 mg (S/Rh = 1000); Solvent: 2-propanol (6 mL); T = 80 °C. [b] Data determined by GC (%) using *n*-undecane as internal standard; [c] r = recycling experiment; " = same value as above.

A comparative experiment was performed using both synthesized and commercial Rh catalysts under identical operating conditions (S/Rh molar ratio = 500/1, 80 °C, 0.2 MPa H_2, 6 h (Table 16 and Figure 5). All Rh-based catalysts tested were completely selective to (VII), with no detectable formation of undesired byproducts such as 4-hydroxypentanoic acid or products arising from further hydrogenation. This exclusive selectivity is advantageous because it substantially simplifies downstream purification. Among the tested catalysts, synthesized Rh/Al_2O_3 (Rh 0.18% *w*/*w*) exhibited the highest activity (78% conversion), surpassing commercial Rh/Al_2O_3 (Rh 5% *w*/*w*; 61% conversion). At constant support chemistry, this difference is plausibly attributable to the preparation protocol, which may yield improved dispersion and a more uniform distribution of the Rh phase; differences in the specific alumina grade may also influence activity. In contrast, synthesized Rh/TiO_2 (Rh 0.15% *w*/*w*) was the least active under these mild-pressure conditions, suggesting that the support can significantly affect metal dispersion and accessible surface area. Similarly, the low conversion obtained with commercial Rh/C (Rh 5% *w*/*w*) is consistent with limited availability of active sites under the chosen conditions.

Table 16. Catalytic performance of synthesized and commercial supported Rh catalysts in the hydrogenation of levulinic acid (VI).

Entry [a]	Cat.	Conversion (%) [b]	VII Selectivity (%) [b]
1	Rh/Al_2O_3 (0.18%)	78	100
2	Rh/TiO_2 (0.15%)	21	100
3	Rh/Al_2O_3 (5%)	61	100
4	Rh/C (5%)	34	100

[a] Reaction conditions: Substrate (VI) 1.07 mmol (0.125 g); Substrate/Rh molar ratio = 500/1Solvent: 2-propanol (6 mL); T = 80 °C; $p(H_2)$ = 0.2 MPa; t = 6h. [b] Data determined by GC (%) using *n*-undecane as internal standard.

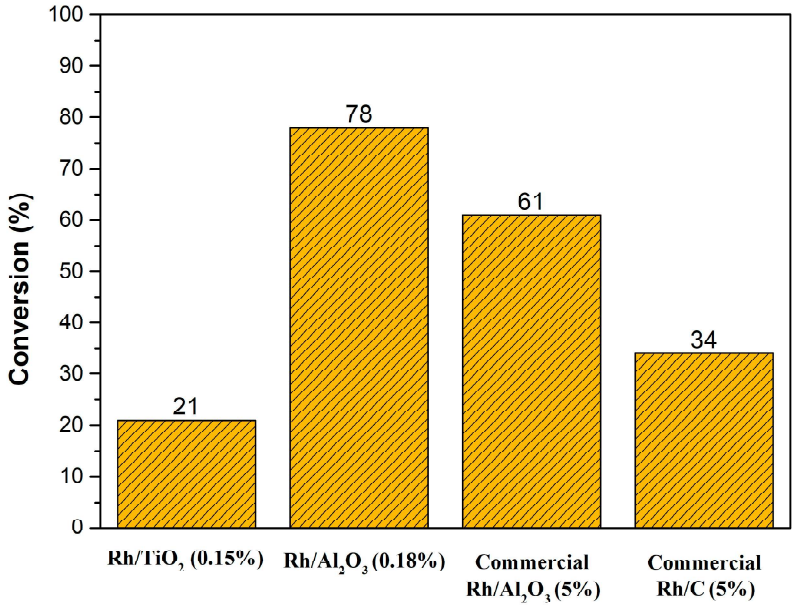

Figure 5. Comparison of catalytic performance of synthesized and commercial supported Rh catalysts in the hydrogenation of levulinic acid (VI).

4. Conclusive Remarks

This work focused on the development and evaluation of low-precious-metal heterogeneous catalysts for hydrogenation reactions, specifically Pd- and Rh-based systems supported on different metal oxides: Pd/Al_2O_3 (Pd 0.24% *w*/*w*), Pd/TiO_2 (Pd 0.18 wt% Pd), Pd/ZrO_2 (Pd 0.21% *w*/*w*), Pd/SiO_2 (Pd 0.37% *w*/*w*), Rh/Al_2O_3 (Rh 0.18% *w*/*w*), and Rh/TiO_2 (Rh 0.15% *w*/*w*). A one-pot synthetic methodology, advantageous due to the avoidance of conventional calcination and activation steps, enabled the successful incorporation of low metal loadings on alumina, titania, zirconia, and silica supports. Catalytic performance was assessed using model substrates containing C=C and/or C=O functionalities, namely *(E)*-cinnamaldehyde and levulinic acid. In the hydrogenation of *(E)*-cinnamaldehyde, Pd catalysts proved highly effective for chemoselective C=C reduction, affording 3-phenylpropanal as the major product. While Pd/ZrO_2 and Pd/SiO_2 exhibited limited activity, Pd/Al_2O_3 and, in particular, Pd/TiO_2 delivered high conversions under relatively mild conditions (0.1–1.0 MPa H_2, 30–60 °C). Pd/Al_2O_3 displayed activity comparable to commercial Pd/Al_2O_3 (2 wt% Pd). Notably, Pd/TiO_2 outperformed not only commercial Pd/Al_2O_3 but also Pd/C (5 wt% Pd), combining higher activity with improved stability upon recycling and enabling full conversion even at high substrate-to-metal ratios (up to 5000/1; 40 °C, 0.2 MPa H_2, 3 h). Support acidity significantly influenced selectivity, most clearly for TiO_2-based catalysts. Acidic surface sites promoted secondary reactions leading to isopropyl 3-phenylpropyl ether and,

more prominently, hemiacetal formation via reaction between 3-phenylpropanal and 2-propanol. Solvent screening confirmed the suitability of a polar protic medium (2-propanol) for these systems; CPME also performed well with Pd/Al_2O_3, although its higher cost limited its practical attractiveness. Rh-based heterogeneous catalysts were also competent for cinnamaldehyde hydrogenation, albeit requiring more forcing conditions to reach quantitative conversion. Rh/TiO_2 was more active than commercial Rh/Al_2O_3 (5 wt% Rh) and Rh/C (5 wt% Rh), but the acidic support again favored hemiacetal formation. In contrast, the synthesized Rh/Al_2O_3 catalyst displayed higher activity and excellent chemoselectivity for C=C hydrogenation, affording 3-phenylpropanal with selectivities above 98%. In levulinic acid hydrogenation, Pd-supported catalysts were essentially inactive toward reduction of the C=O group, even under relatively harsh conditions (80 °C, 2.0 MPa H_2). Conversely, Rh/TiO_2 and Rh/Al_2O_3 showed substantially improved performance and surpassed commercial Rh benchmarks. The alumina-supported Rh catalyst was the most active system investigated. A key outcome of these Rh catalysts was their complete selectivity toward γ-valerolactone, a high-value product of interest as a fuel component, synthetic intermediate, and green solvent. Overall, the results demonstrate progress toward sustainable catalyst design by combining high catalytic performance and, in several cases, good recyclability with minimal loadings of precious metals. This strategy offers both economic benefits and reduced reliance on scarce resources, aligning with the principles of green chemistry and sustainable technologies.

Outlook

Future work should include the following: (i) advanced structural characterization of the catalysts by XANES and EXAFS; (ii) evaluation of additional model substrates to probe versatility in hydrogenation of different functional groups; and (iii) extension of the one-pot methodology to new heterogeneous platforms, including supports widely used in industry, such as magnetite.

Supplementary Materials: The following supporting information can be downloaded at: https://www.mdpi.com/article/10.3390/reactions7030039/s1, Figure S1: SEM (Scanning Electron Microscopy) micrographs of homemade TiO_2; Figure S2: SEM micrographs of commercial TiO_2; Figure S3: SEM and EDX (Energy-Dispersive X-ray) analyses of Pd/TiO_2 (commercial support); Figure S4: SEM micrographs of Pd/TiO_2 (commercial support); Figure S5: SEM micrographs of Pd/TiO_2 (homemade): (left) In-Lens and (right) backscattered electron detector images; Figure S6: SEM and EDX analyses of Pd/TiO_2 (homemade support); Figure S7: SEM and EDX analyses of Rh/TiO_2; Figure S8: STEM (Scanning Transmission Electron Microscopy) image of Rh/TiO_2; Figure S9: STEM image of Pd/TiO_2 (commercial support); Figure S10: STEM image of Pd/TiO_2 (homemade support); Figure S11: SEM images of Pd/Al_2O_3: A (before use); B (after use); C (magnified view of selected clusters after use); Figure S12: TEM (Transmission Electron Microscopy) images of Rh/Al_2O_3: (a) overall view; (b) and (c): magnified view of selected clusters; (d) magnified view of selected clusters after use.

Author Contributions: S.P.: conceptualization, supervision, investigation, formal analysis, writing—original draft, and writing—review and editing; L.S.: investigation, methodology; A.D.M.: investigation, methodology; O.P.: conceptualization, supervision, writing—original draft. All authors have read and agreed to the published version of the manuscript.

Funding: This research received no external funding.

Data Availability Statement: The original contributions presented in this study are included in the article and supplementary material. Further inquiries can be directed to the corresponding author.

Acknowledgments: The authors express their gratitude to Chimet for providing alumina.

Conflicts of Interest: The authors declare no conflicts of interest.

https://doi.org/10.3390/reactions7030039

References

1. Hutchings, G.J.; Wells, R.P.K.; Bailie, J.E. Heterogeneous catalytic hydrogenation. *Sci. Prog.* **1999**, *82*, 233–250.
2. Nishimura, S. *Handbook of Heterogeneous Catalytic Hydrogenation for Organic Synthesis*, 1st ed.; Wiley-Interscience: New York, NY, USA, 2001.
3. Deutschmann, O.; Knözinger, H.; Kochloefl, K.; Turek, T. Heterogeneous Catalysis and Solid Catalysts. In *Ullmann's Encyclopedia of Industrial Chemistry*; Wiley-VCH: Weinheim, Germany, 2009.
4. Thomas, J.M.; Thomas, W.J. *Principles and Practice of Heterogeneous Catalysis*, 2nd ed.; Wiley-VCH: Weinheim, Germany, 2015.
5. Deng, D.; Novoselov, K.S.; Fu, Q.; Zheng, N.; Tian, Z.; Qiao, S.-Z. Catalysts and Mechanisms for the Selective Heterogeneous Hydrogenation of Small Molecules. *Chem. Rev.* **2020**, *120*, 11075–11141.
6. Davies, T.E.; Williams, C.T. Metal Oxide Supports in Heterogeneous Catalysis: Properties and Tunability. *Appl. Catal. A* **2023**, *635*, 118390.
7. Bagheri, S.; Abd Hamid, S.B.; Muhd Julkapli, N.; Vorontsov, A. Titanium Dioxide as a Catalyst Support in Heterogeneous Catalysis. *Sci. World J.* **2014**, *2014*, 727496.
8. Sebastian, J.; Mebrahtu, C.; Zeng, F.; Palkovits, R. Strong Metal-Support Interactions on TiO_2-Supported Metal Catalysts for Fine-Tuning Catalysis. *Angew. Chem. Int. Ed.* **2026**, *65*, e02611.
9. Yu, X.; Williams, C.T. Recent advances in the applications of mesoporous silica in heterogeneous catalysis. *Catal. Sci. Technol.* **2022**, *12*, 5765–5794.
10. Monguchi, Y.; Sajiki, H.; Ichikawa, T. Recent development of palladium-supported catalysts for chemoselective hydrogenation. *Chem. Pharm. Bull.* **2017**, *65*, 2–9.
11. Trueba, M.; Trasatti, S.P. γ-Alumina as support for catalysts: A review of fundamental aspects. *Eur. J. Inorg. Chem.* **2005**, *2005*, 3393–3403.
12. Leybo, D.C.; Etim, U.J.; Monai, M.; Bare, S.R.; Zhong, Z.; Vogt, C. Metal-Support Interactions in Metal Oxide-Supported Atomic, Cluster, and Nanoparticle Catalysis. *Chem. Soc. Rev.* **2024**, *53*, 10450–10490.
13. Wang, H.; Gao, Z.; Sun, B.; Mu, S.; Dang, F.; Guo, X.; Ma, D.; Shi, C. Engineering Metal-Support Interaction to Construct Catalytic Interfaces and Redisperse Metal Nanoparticles. *Chem Catal.* **2023**, *3*, 100768.
14. Zhou, J.E.; Gao, Z.; Xiang, G.; Zhai, T.; Liu, Z.; Zhao, W.; Liang, X.; Wang, L. Interfacial Compatibility Critically Controls Ru/TiO_2 Metal-Support Interaction Modes in CO_2 Hydrogenation. *Nat. Commun.* **2022**, *13*, 327.
15. Kozyr, E.; Paciok, P.; Janssens, K.; Lagostina, V.; Pellegrini, R.; Usoltsev, O.; Skorynina, A.; Chiesa, M.; De Vos, D.; Groppo, E.; et al. Origin of the Strong Metal-Support Interaction in Pd/TiO_2. *J. Catal.* **2025**, *452*, 116448.
16. Chen, H.; Yang, Z.; Wang, X.; Polo-Garzon, F.; Halstenberg, P.W.; Wang, T.; Suo, X.; Yang, S.-Z.; Meyer, H.M.; Wu, Z.; et al. Photoinduced Strong Metal-Support Interaction for Enhanced Catalysis. *J. Am. Chem. Soc.* **2021**, *143*, 8521–8526.
17. Qi, F.; Peng, J.; Liang, Z.; Guo, J.; Liu, J.; Fang, T.; Mao, H. Strong Metal-Support Interaction (SMSI) in Environmental Catalysis: Mechanisms, Application, Regulation Strategies, and Breakthroughs. *Environ. Sci. Ecotechnol.* **2024**, *22*, 100443.
18. Scotti, N.; Bossola, F.; Zaccheria, F.; Ravasio, N. Copper–Zirconia catalysts: Powerful multifunctional catalytic tools to approach sustainable processes. *Catalysts* **2020**, *10*, 168.
19. Wheng, J.-W. Palladium-catalyzed olefin isomerization reactions. *Eng. Technol. Trends* **2025**, *3*, 51–59.
20. Nieuwenhuys, B.E.; Siera, J.; Wolf, R.M.; van Delft, F.C.M.J.M. Composition and properties of platinum-rhodium alloy surfaces. *ISIJ Int.* **1989**, *29*, 550–559.
21. Jiang, R.; Wang, H.; Liu, L.; Geng, B.; Chu, X.; Shi, Y.; Wang, X.; Song, S.; Zhang, H. Recent progress of Rh-based three-way catalysts. *Smart Mol.* **2024**, *2*, e20240004.
22. Paganelli, S.; Angi, A.; Pajer, N.; Piccolo, O. A smart heterogeneous catalyst for efficient, chemo- and stereoselective hydrogenation of 3-hexyn-1-ol. *Catalysts* **2021**, *11*, 14.
23. Piccolo, O.; Arčon, I.; Das, G.; Aquilanti, G.; Prai, A.; Paganelli, S.; Facchin, M.; Beghetto, V. Synthesis of Helional by hydrodechlorination reaction in the presence of mono and bi-metallic catalysts supported on alumina. *Catalysts* **2024**, *14*, 255.
24. Paganelli, S.; D'Acunzi, C.; Riela, S.; Massaro, M.; Di Michele, A.; Muzzi, B.; Piccolo, O. Selective Hydrogenation of Citral: A Catalytic Challenge. *Mol. Catal.* **2026**, *593*, 115765.
25. Patil, K.N.; Manikanta, P.; Srinivasappa, P.M.; Jadhav, A.H.; Nagaraja, B.M. State-of-the-art and perspectives in transition metal-based heterogeneous catalysis for selective hydrogenation of cinnamaldehyde. *J. Environ. Chem. Eng.* **2023**, *11*, 109168.
26. Kahsar, K.R.; Johnson, S.; Schwartz, D.K.; Medlin, J.W. Hydrogenation of Cinnamaldehyde over Pd/Al_2O_3 Catalysts Modified with Thiol Monolayers. *Top. Catal.* **2014**, *57*, 1505–1511.

27. Shimizu, T.; Ota, M.; Sato, Y.; Inomata, H. Effect of pore structure on catalytic properties of mesoporous silica supported rhodium catalysts for the hydrogenation of cinnamaldehyde. *Chem. Eng. Res. Des.* **2015**, *104*, 174–179.
28. Patil, K.N.; Prasad, D.; Bhanushali, J.T.; Kakade, B.; Jadhav, A.H.; Nagaraja, B.M. Chemoselective hydrogenation of cinnamaldehyde over a tailored oxygen-vacancy-rich Pd@ZrO_2 catalyst. *New J. Chem.* **2021**, *45*, 5659–5681.
29. Li, Z.; Leng, L.; Lu, X.; Zhang, M.; Xu, Q.; Horton, J.H.; Zhu, J. Single palladium atoms stabilized by β-FeOOH nanorod with superior performance for selective hydrogenation of cinnamaldehyde. *NanoResearch* **2022**, *15*, 3114–3121.
30. Magubane, A.; Gangatharan, P.M.; Mente, P.; Phaahlamohlaka, T.N.; Maubane-Nkadimeng, M.S.; Lee, M.; O'Connell, J.; Coville, N.J. Hydrogenation of Cinnamaldehyde Using Carbon Dots Reduced Palladium Nanoparticles. *Catal. Lett*. **2024**, *154*, 3212–3224.
31. Shi, H.; Su, T.; Qin, Z.; Ji, H. Role of catalyst surface-active sites in the hydrogenation of *α,β*-unsaturated aldehyde. *Front. Chem. Sci. Eng*. **2024**, *18*, 64.
32. Pitínová, M.; Danylo, I.; Shafiq, A.; Hartman, T.; Khover, M.; Sevemez, B.; Koláčný, L.; Veselý, M. Graphene Oxide-Supported Metal Catalysts for Selective Hydrogenation of Cinnamaldehyde: Impact of Metal Choice and Support Structure. *Catalysts* **2025**, *15*, 470.
33. Serrano-Ruiz, J.C.; Dumesic, J.A. Biomass Conversion to Fuels. *Energy Environ. Sci.* **2011**, *4*, 83–99.
34. Besson, M.; Gallezot, P.; Pinel, C. Conversion of Biomass into Chemicals over Metal Catalysts. *Chem. Rev.* **2014**, *114*, 1827–1870.
35. Signoretto, M.; Taghavi, S.; Ghedini, E.; Menegazzo, F. Catalytic Production of Levulinic Acid (LA) from Actual Biomass. *Molecules* **2019**, *24*, 2760.
36. Yan, K.; Yang, Y.; Chai, J.; Lu, Y. Catalytic Reactions of Gamma-Valerolactone: A Platform to Fuels and Value-Added Chemicals. *Appl. Catal. B* **2015**, *179,* 292–304.
37. Wright, W.R.H.; Palkovits, R. Development of Heterogeneous Catalysts for the Conversion of Levulinic Acid to Gamma-Valerolactone. *ChemSusChem* **2012**, *5,* 1657–1667.
38. Alonso, D.M.; Wettstein, S.G.; Dumesic, J.A. Efficient Conversion of Levulinic Acid into γ-Valerolactone over Metal Catalysts. *ChemSusChem* **2010**, *3*, 1142–1145.
39. Upare, P.P.; Lee, J.-M.; Hwang, D.W.; Halligudi, S.B.; Hwang, Y.K.; Chang, J.-S. Selective Hydrogenation of Levulinic Acid to γ-Valerolactone over Carbon-Supported Noble Metal Catalysts. *J. Ind. Eng. Chem.* **2011**, *17*, 287–292.
40. Obregón, I.; Gandarias, I.; Al-Shaal, M.G.; Mevissen, C.; Arias, P.L.; Palkovits, R. The Role of the Hydrogen Source on the Selective Production of γ-Valerolactone and 2-Methyltetrahydrofuran from Levulinic Acid. *ChemSusChem* **2016**, *9*, 2488–2495.
41. Ruiz-Bernal, Z.; Tane, E.G.; Sánchez-Lozano, J.; Rives-López, J.M.; Román-Martínez, M.C.; Lillo-Ródenas, M.A. The Relevant Role of TiO_2 for Enhancing the Ru/TiO_2-Catalyzed Conversion of Levulinic Acid to γ-Valerolactone. *Catal. Today* **2025**, *458*, 115375.
42. Ruiz-Bernal, Z.; Lillo-Ródenas, M.A.; Román-Martínez, M.C. Ru Catalysts Supported on Commercial and Biomass-Derived Activated Carbons. *Catalysts* **2021**, *11*, 559.
43. Khalid, M.; Granollers Mesa, M.; Scapens, D.; Osatiashtiani, A. Advances in Sustainable γ-Valerolactone Production via Catalytic Transfer Hydrogenation of Levulinic Acid and Its Esters. *ACS Sustain. Chem. Eng*. **2024**, *12*, 16494–16517.
44. Ftouni, J.; Genuino, H.C.; Muñoz-Murillo, A.; Bruijnincx, P.C.A.; Weckhuysen, B.M. Influence of Sulfuric Acid on the Performance of Ruthenium-Based Catalysts in the Liquid-Phase Hydrogenation of Levulinic Acid. *ChemSusChem* **2017**, *10*, 2891–2896.
45. Tan, J.; Cui, J.; Ding, G.; Deng, T.; Zhu, Y.; Li, Y. Efficient Aqueous Hydrogenation of Levulinic Acid to γ-Valerolactone over a Highly Active and Stable Ruthenium Catalyst. *Catal. Sci. Technol.* **2016**, *7*, 1469–1475.
46. Anjali, K.; Venkatesha, N.J.; Christopher, J.; Sakthivel, A. Rhodium Porphyrin Molecule-Based Catalysts for the Hydrogenation of Levulinic Acid to γ-Valerolactone. *New J. Chem.* **2020**, *44*, 1164–1175.
47. Li, M.; Li, G.; Li, N.; Wang, A.; Dong, W.; Wang, X.; Cong, Y. Aqueous Phase Hydrogenation of Levulinic Acid to 1,4-Pentanediol. *Chem. Commun.* **2014**, *50*, 1414–1416.
48. Wang, X.; Qi, X.; Qiu, M.; Shen, F.; Yang, J.; Shen, B. Bimetallic Ordered Mesoporous Carbon from Lignin for Catalytic Selective Hydrogenation of Levulinic Acid. *Fuel* **2023**, *341*, 127720.
49. Tang, Y.; Fu, J.; Wang, Y.; Guo, H.; Qi, X. Bimetallic Ni–Zn@OMC Catalyst for Selective Hydrogenation of Levulinic Acid. *Fuel Process. Technol.* **2023**, *240*, 107559.
50. García-Sancho, C.; Mérida-Robles, J.M.; Cecilia-Buenestado, J.A.; Moreno-Tost, R.; Maireles-Torres, P.J. The Role of Copper in the Hydrogenation of Furfural and Levulinic Acid. *Int. J. Mol. Sci.* **2023**, *24*, 2443.
51. Xu, Y.; Liang, Y.; Guo, H.; Qi, X. Catalytic Hydrogenation of Levulinic Acid over Lignin-Metal Coordinated Carbon Nanospheres. *Int. J. Biol. Macromol.* **2023**, *240*, 124451.

52. Yuan, Q.; van de Bovenkamp, H.H.; Zhang, Z.; Piskun, A.S.; Sami, S.; Havenith, R.W.A.; Heeres, H.J.; Deuss, P.J. Mechanistic Investigations into the Catalytic Levulinic Acid Hydrogenation, Insight in H/D Exchange Pathways, and a Synthetic Route to d_8-γ-Valerolactone. *ACS Catal.* **2021**, *11*, 10467–10477.
53. Chen, X.; Mao, S.S. Titanium Dioxide Nanomaterials: Synthesis, Properties, Modifications, and Applications. *Chem. Rev.* **2007**, *107*, 2891–2959.